

HEXAFERRITES - SINGLE PHASE MAGNETO-ELECTRIC MULTIFERROICS

Tatyana Koutzarova¹, Svetoslav Kolev^{1,2}, Kiril Krezhov¹, Borislava Georgieva¹,
Chavdar Ghelev¹, Todor Cholakov², Lan Maria Tran³, Michal Babij³

¹Institute of Electronics, Bulgarian Academy of Sciences
72 Tsarigradsko Chaussee, Sofia 1784, Bulgaria

²Neofit Rilski South-Western University, 66 Ivan Mihailov St.
Blagoevgrad 2700, Bulgaria

³Institute of Low Temperature and Structure Research
Polish Academy of Sciences, 2 Ul. Okólna, Wrocław 50-422, Poland
E-mail: tanya@ie.bas.bg

Received 20 September 2023

Accepted 23 May 2024

DOI: 10.59957/jctm.v59.i4.2024.29

ABSTRACT

Multiferroic materials are an exceptional class of magnetic materials where long-range magnetic and ferroelectric orders coexist, thus provoking the researchers' interest from both basic and practical points of view. The magneto-electric multiferroics are materials that combine coupled electric and magnetic dipoles. Recently, research has focused on the occurrence of the magnetoelectric effect in some hexagonal ferrite types and the possibility of their use as single-phase multiferroic and magnetoelectric materials. For many years, various hexaferrites have been intensively studied as materials for permanent magnets, high-density recording media, microwave devices, biomedical applications, etc. The magnetic structure and especially the specific magnetic spin arrangement under certain conditions proved to be key factors for the realization of magneto-electric phases in hexaferrites. Here some recent advances in our studies of the magnetic phase transitions in the Y-type hexaferrites are overviewed. In particular, the influence of the replacement of non-magnetic Me^{2+} cations with magnetic cations and of magnetic Fe^{3+} cations with non-magnetic ones on the magnetic properties and occurring magnetic phase transitions in Y-type hexaferrites are exemplified with $Ba_{0.5}Sr_{1.5}Zn_2Fe_{12}O_{22}$.

Keywords: hexaferrites, magnetic phase transition, magnetic properties.

INTRODUCTION

The multiferroics are multifunctional materials where two or more of the primary ferroic properties (ferromagnetism, ferroelectricity, ferroelasticity, ferrotoroidicity) coexist [1]. The interest in magnetoelectric multiferroic materials in which ferroelectricity and ferromagnetism exist is due to possible clearly manifested coupling effects between magnetic and electrical properties. The magneto-electric effect allows one to manipulate the magnetic phase by an external electrical field and/or manipulate the electric phase by an external magnetic field [2]. This cross-coupling effect (magneto-electric effect) gives additional functionality to materials and opens new possibilities in spintronics. It can be exploited in both novel and in well-

known devices, e.g., four-stage logic memory devices, photovoltaic multiferroic solar cells, multiferroic gyrators, electrical-field-controlled spintronic devices, *ac/dc* magnetic field sensors, electrical and magnetic field sensors in biomedicine, electric power generators; and in electrical-field-controlled microwave components, such as phase shifters, filters and switches for wireless technologies at up to terahertz frequencies, an area that is essentially unexplored. From the practical point of view of using multiferroics in multifunctional devices, it is important to control the electrical polarization or dielectric constant using weak magnetic fields or to manipulate the magnetization by an *E* field at temperatures near and above room temperature. The research has been focused mainly on three types of multiferroics – composites containing ferroelectric and

ferromagnetic materials and single-phase multiferroics containing ferroelectric materials doped with metal cations; and ferrites with spiral ordering of the magnetic moments, like hexaferrites, which are the subject of our study.

The hexaferrites were discovered in the 1950s and became a subject of interest in solid-state science due to their rich crystal chemistry and a complex structural topology [3]. The most important members of the hexaferrites family are summarized in Table 1; the magneto-electric effect, which is of application interest, is observed in M, Y, Z and U-type hexaferrites. T. Kimura and co-authors were the first to report a measurable magnetoelectric effect in hexaferrites when studying a single crystal of $\text{Ba}_{0.5}\text{Sr}_{1.5}\text{Zn}_2\text{Fe}_{12}\text{O}_{22}$ (Y-type hexaferrite) in a field of about 1 T and at a temperature close to room temperature, the effect being significant at $T < 130$ K [4, 5]. Kimura et al. [4] described the existence of the screw magnetic structure in the absence of a magnetic field that is incommensurately modulated by low magnetic fields, three intermediate structures commensurately modulated by the magnetic field and, finally, a collinear ferrimagnetic structure that is formed at 2.2 T, all obtainable at room temperature. Magneto-electric coupling was observed in the Intermediate III phase with $\bar{3}'_m$ magnetic symmetry and appeared on the M - H curves as a plateau with a different slope between 0.3 T and 2.2 T. Between these values of the magnetic field, the electric polarization at 10 K reached a maximum of $150 \mu\text{C m}^{-2}$.

The Y-type hexaferrites have a rhombohedral space group $R(-3m)$ crystal structure (Fig. 1). The structure can be described as consisting of two types of blocks - S- and T-, consecutively stacked along the hexagonal c axis in the sequence (TST'ST'S'), with the primes

indicating rotation about the c -axis by 120 degrees [6]. The hexagonal unit cell contains 18 oxygen layers. The S-block ($\text{Me}_2\text{Fe}_4\text{O}_8$; spinel block) can be thought of as a double spinel layer. It contains two spinel units of two layers of four oxygen atoms with three metal atoms between each layer in four octahedral sites and two tetrahedral sites [6]. Thus, there are six sites for metals, four of them octahedral and two tetrahedral. The T-block ($\text{Ba}_2\text{Fe}_8\text{O}_{14}$) is made up of four oxygen layers, with a barium atom substituting an oxygen atom in the inner two layers, which are opposite one another in the neighboring layers, resulting in two tetrahedral and six octahedral sites [6]. All cations (Me^{+2} and Fe^{+3}) are located in six special Wyckoff positions: two tetrahedral sites (6_{cIV} and $6_{\text{c*IV}}$) and four octahedral sites (3_{aVI} , 3_{bVI} , 6_{cVI} and 18_{hVI}). Two octahedral sites are in the T-block and one is in the S-block, and one octahedral site h with the highest multiplicity is common for both the T-and S-block. For example, the Mg^{2+} ions occupy randomly tetrahedral and octahedral sites in $\text{Ba}_2\text{Mg}_2\text{Fe}_{12}\text{O}_{22}$ [7], whereas the Zn^{2+} cations prefer to occupy tetrahedral sites, together with the Fe^{3+} cations [8]. To understand and design magnetic and other physical properties, it is necessary to have information on the crystal structure of the material, the ionic distributions, and the interactions between cations at different sites.

The earliest considerations regarding the possible spin arrangement in the Y-type hexaferrite structure date as far back as the 1950s [3]. Using a qualitative approach and magnetic data, Gorter predicted the orientation of the magnetic moments in the Y-type ferrite sublattices and the relative strength of the superexchange interactions [9]. The easy magnetization axis lies in a plane perpendicular to the c -axis, while the non-compensated magnetic moment lying in the ab plane arises from

Table 1. Hexaferrites - molecular formula, structural blocks.

Type	Molecular formula	Hexaferrite blocks	Magnetoelectric effect
M	$\text{BaFe}_{12}\text{O}_{19}$	RSR*S*	$\text{BaFe}_{12-x}\text{Sc}_x\text{Mg}_8\text{O}_{19}$
W	$\text{BaMe}_2\text{Fe}_{16}\text{O}_{27}$	$\text{RS}_2\text{R}^*\text{S}^*_2$	
X	$\text{Ba}_2\text{Me}_2\text{Fe}_{28}\text{O}_{46}$	$(\text{RSR}^*\text{S}^*_2)_3$	
Y	$\text{Ba}_2\text{Me}_2\text{Fe}_{12}\text{O}_{22}$	$(\text{TS})_3$	$\text{Ba}_2\text{Mg}_2\text{Fe}_{12}\text{O}_{22}$, $\text{Ba}_{0.5}\text{Sr}_{1.5}\text{Zn}_2\text{Fe}_{12}\text{O}_{22}$, $\text{Ba}_{0.5}\text{Sr}_{1.5}\text{Zn}_2\text{Fe}_{11-x}\text{Al}_x\text{O}_{22}$
Z	$\text{Ba}_3\text{Me}_2\text{Fe}_{24}\text{O}_{41}$	RSTSR*S*T*S*	$\text{Sr}_3\text{Co}_2\text{Fe}_{24}\text{O}_{41}$
U	$\text{Ba}_4\text{Me}_2\text{Fe}_{36}\text{O}_{60}$	RSR*S*T*S*	$\text{Sr}_4\text{Co}_2\text{Fe}_{36}\text{O}_{60}$

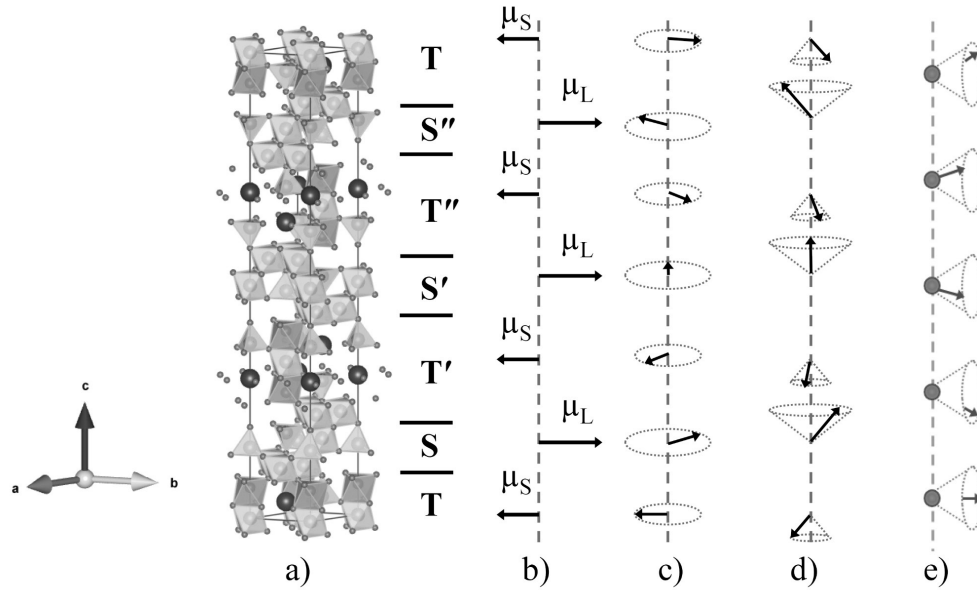


Fig. 1. (a) Schematic crystal structure of Y-type hexaferrite; (b) the collinear ferrimagnetic structure consists of alternate stacks of two spin blocks with μ_L (larger magnetic moments) and μ_S (smaller magnetic moments) along the c axis. (c) and (d) [26] represent the non-polar spin order phases with propagation vector k_0 parallel to c -axis: proper screw (PS) and alternate longitudinal conical (ALC) structure, respectively, exhibited at lower temperatures, (e) the transverse conical structure sensitive to external magnetic field.

dominating majority spins in octahedral $3a$, $3b$, and $18h$ sites, and minority spins in tetrahedral $6c_T$ and $6c_S$ and octahedral $6c$ sites. These majority and minority spins determine two magnetic sublattices – L_m and S_m , correspondingly, opposite large and small magnetization (Fig. 1) [7]. The magnetic sublattices are different from the crystal structural blocks and are alternating along [001]. Taking into consideration these two sublattices, L_m and S_m , helps one understand the magnetic structures of the Y-type hexaferrites. The superexchange interaction across the boundary of the sublattices, Fe(4)-O(2)-Fe(5), can be affected by a proper substitution. Therefore, the T block, which contains the Fe(4)-O(2)-Fe(5) bonds, is essential to bringing into being the non-collinear screw structure in the Y-type hexaferrite [10].

Research has shown that not only does the substitution of iron cations in these two positions affect the magnetic ordering, but also whether the Me^{2+} cations are magnetic or nonmagnetic, which positions they prefer - octahedral or tetrahedral, and last but not least, oxygen defects, since the superexchange interaction between the magnetic cations is through the oxygen atoms. It was found that the partial replacement of Ba^{2+}

with Sr^{2+} (smaller ionic radius), causing a distortion in the crystal cell, leads to the redistribution of Zn^{2+} and Fe^{3+} in the tetrahedral sites and change in the magnetic spin arrangement. The turn angle is between 0° and 180° for $1 < x < 1.6$ in $Ba_{2-x}Sr_xZn_2Fe_{12}O_{22}$ leading to a helical spin ordering. For example, the $Ba_{0.5}Sr_{1.5}Zn_2Fe_{12}O_{22}$ shows a helical spin ordering where the spin moments lie and rotate in the ab -plane below 326 K (Néel temperature) [11]. Detailed descriptions of the crystal and magnetic structures were given in [12, 13]. Applying a magnetic field perpendicular to the c -axis induces different intermediate magnetic phases forming a slightly modified helix at low field to a collinear ferromagnetic phase at high field. The appearance of a helicoidal or a conical spin ordering is a prerequisite for the existence of the magneto-electric effect in Y-type hexaferrites; this is why studying the effect of different metal cations substitutions on the crystal and magnetic structures is of particular importance. Thus, Hirose et al. were able to achieve control of magnetization by an electric field up to 325 K in oriented polycrystalline $BaSrCo_2Fe_{11}AlO_{22}$ [14]. Conversely, by applying a magnetic field they also reported an induced electric polarization of $140 \mu C m^{-2}$

at 200 K and $51 \mu\text{C m}^{-2}$ at 300 K.

Among the methods for the synthesis of Y-type hexaferrites, the solid-state reaction [15, 16] and the sol-gel auto-combustion method [17, 18] are most often applied. In the following, our results on the impact of partial replacement of magnetic Fe^{3+} cations with nonmagnetic ones and of nonmagnetic Zn^{2+} with magnetic cations in $\text{Ba}_{0.5}\text{Sr}_{1.5}\text{Zn}_2\text{Fe}_{12}\text{O}_{22}$ are summarized and compared with evidence provided in the literature. The influence of preferred site occupancy by a given cation on the adopted crystal and magnetic structures is also considered.

EXPERIMENTAL

The citric acid sol-gel auto-combustion was used for synthesis of Y-type hexaferrites. Specific details of the procedure were described in our earlier papers [19 - 21]. The metal cations (usually nitrates are used) and citric-acid (in form of solution) form stable complexes and prevent precipitation of oxides or oxyhydroxides in the solution. As the metal citrates are stable without precipitation at $\text{pH} = 7 - 8$, ammonia solution is usually added. The solution is heated at 120°C resulting in slow evaporation and formation of a gel mass. During the dehydration process, the gel-like substance self-ignites. The auto-combustion is accompanied by an oxidation-reduction exothermic reaction, with the heat released being sufficient to form an oxide mixture. The as-prepared auto-combusted powders are usually heat-treated at temperatures below 850°C to completely remove residual organic precursors. The final process is calcination of the resulting powders at 1170°C to obtain Y-type hexaferrites, which in our case were $\text{Sr}_{1.5}\text{Ba}_{0.5}\text{Zn}_2\text{Fe}_{12}\text{O}_{22}$, $\text{Sr}_{1.5}\text{Ba}_{0.5}\text{Zn}_2\text{Fe}_{11.92}\text{Al}_{0.08}\text{O}_{22}$, $\text{Ba}_{0.5}\text{Sr}_{1.5}\text{NiZnFe}_{12}\text{O}_{22}$ and $\text{Ba}_{0.5}\text{Sr}_{1.5}\text{NiMgFe}_{12}\text{O}_{22}$.

The magnetic parameters were measured using a commercial physical-property-measurement-system (PPMS) (Quantum Design) equipped with an ACMS option. Magnetic hysteresis loops were taken at 4.2 K and 300 K. The changes in the magnetization as a function of temperature (from 4.2 K to 300 K) in zero-field-cooled (ZFC) and field-cooled (FC) protocols were followed in magnetic fields of 100 Oe and 500 Oe. In the ZFC procedure, the sample studied was cooled down from room temperature to 4.2 K in the absence of magnetic field; then, the magnetization was recorded as

the temperature was increased from 4.2 K to 300 K at the rate of 3 K min^{-1} in the magnetic field applied. The FC curve was obtained as the sample was cooled from 300 K to 4.2 K in the same magnetic field.

RESULTS AND DISCUSSION

Here we present our results on the magnetic properties of polycrystalline materials from the point of view of magnetic-phase transitions. Y-type hexaferrites have an easy axis lying in the *ab* plane, therefore the hysteresis loops are very narrow, and the coercive field is accordingly rather small. Typically, the coercive field (H_c) is from a few Oe to 200 Oe. The measured values for the synthesized by us materials are summarized in Table 2. The saturation magnetization (M_s) value is between 20 emu g^{-1} and 40 emu g^{-1} at room temperature.

When one investigates the magnetic properties, the first indicator of a magnetic phase transition or spin rearrangement is the observation of a step-like behavior in the initial magnetization curves or a multistage hysteresis loop (Fig. 2a). The multistage hysteresis curve in a low magnetic field is very often observed when two magnetic states with different magnetic moments ordering are present simultaneously. For example, for $\text{Sr}_{1.5}\text{Ba}_{0.5}\text{Zn}_2\text{Fe}_{11.92}\text{Al}_{0.08}\text{O}_{22}$ and $\text{Ba}_{0.5}\text{Sr}_{1.5}\text{NiMgFe}_{12}\text{O}_{22}$ powder materials, in the region of low magnetic fields the magnetic system undergoes transitions through metamagnetic states, including those between screw spin ordering and conical spin ordering (Fig. 2b) [20]. The change in the magnetic structure affects the magnetization of the specimen and gives rise to the observation of a multistage hysteresis loop. When the non-magnetic Zn^{2+} is half-substituted by the magnetic Ni^{2+} in $\text{Ba}_{0.5}\text{Sr}_{1.5}\text{NiZnFe}_{12}\text{O}_{22}$, the triple hysteresis loop is observed at 4.2 K in the low magnetic field range (Fig. 2c). The appearance of a triple hysteresis loop in the range of low magnetic fields between 1 kOe and -1 kOe points to the existence of an intermediate phase between the proper-screw spin phase and the conical spin one. Kim et al. reported similar behavior at a higher degree of Al-substitution in $\text{Ba}_{0.5}\text{Sr}_{1.5}\text{Ni}_2(\text{Fe}_{0.97}\text{Al}_{0.03})_{12}\text{O}_{22}$ [22].

The magnetic-phase transitions induced by temperature changes when a constant external magnetic field is applied are traced by carrying out the measurements following a zero-field-cooled (ZFC) protocol and a field-cooled (FC) protocol. Fig. 3 shows

Table 2. Magnetic properties of Y-type hexaferrite powders: M_s – saturation magnetization, H_c - coercivity field.

Sample	Temperature, K	M_s , emu/g	H_c , Oe
$\text{Sr}_{1.5}\text{Ba}_{0.5}\text{Zn}_2\text{Fe}_{12}\text{O}_{22}$ [19]	4.2	71	57
$\text{Sr}_{1.5}\text{Ba}_{0.5}\text{Zn}_2\text{Fe}_{12}\text{O}_{22}$ [19]	300	38	18
$\text{Sr}_{1.5}\text{Ba}_{0.5}\text{Zn}_2\text{Fe}_{11.92}\text{Al}_{0.08}\text{O}_{22}$ [20]	4.2	70	32
$\text{Sr}_{1.5}\text{Ba}_{0.5}\text{Zn}_2\text{Fe}_{11.92}\text{Al}_{0.08}\text{O}_{22}$ [20]	300	31	55
$\text{Ba}_{0.5}\text{Sr}_{1.5}\text{NiZnFe}_{12}\text{O}_{22}$ [21]	4.2	54	34
$\text{Ba}_{0.5}\text{Sr}_{1.5}\text{NiZnFe}_{12}\text{O}_{22}$ [23]	300	37	22
$\text{Ba}_{0.5}\text{Sr}_{1.5}\text{NiMgFe}_{12}\text{O}_{22}$ [24]	4.2	32	44
$\text{Ba}_{0.5}\text{Sr}_{1.5}\text{NiMgFe}_{12}\text{O}_{22}$ [24]	300	24	35

the ZFC-FC curves as a function of the temperature in an applied magnetic field of 100 Oe for all synthesized powder samples. The FC curve for $\text{Ba}_{0.5}\text{Sr}_{1.5}\text{Zn}_2\text{Fe}_{12}\text{O}_{22}$ sample decreases monotonically as the temperature is raised. The ZFC curves increase with the temperature and some changes are observed at 74 K and 232 K. The partial substitution of magnetic Fe^{3+} with non-magnetic Al^{3+} provoke changes in the ZFC-curve behavior of $\text{Ba}_{0.5}\text{Sr}_{1.5}\text{Zn}_2\text{Al}_{0.08}\text{Fe}_{11.92}\text{O}_{22}$. The magnetization decreases slowly up to around 285 K and starts growing as the temperature is raised further above 300 K. The minimum exhibited by the ZFC and FC curves at about 285 K is the onset of the magnetic order changing from a proper-screw spin phase to a collinear ferrimagnetic arrangement as the temperature is raised. Accordingly, a helical spin screw magnetic order can be expected below 285 K in this case. When the non-magnetic Zn^{2+} is half substituted by magnetic Ni^{2+} in $\text{Ba}_{0.5}\text{Sr}_{1.5}\text{NiZnFe}_{12}\text{O}_{22}$, the ZFC and FC magnetization curves have a different behavior. The magnetization grows smoothly up to about 200 K; than the increase becomes very quick with the further temperature rise to 300 K. A similar behavior is observed in a $\text{Ba}_{0.5}\text{Sr}_{1.5}\text{NiMgFe}_{12}\text{O}_{22}$ powder sample at 260 K. This indicates that one might expect a change from the screw magnetic ordered state to a ferrimagnetic arrangement through successive metamagnetic transitions and the development of the magnetic structures related to the magnetoelectric effect in accordance with the findings of Hiraoka et al. for $\text{Ba}_{0.5}\text{Sr}_{1.5}\text{Ni}_2\text{Fe}_{12}\text{O}_{22}$ [25].

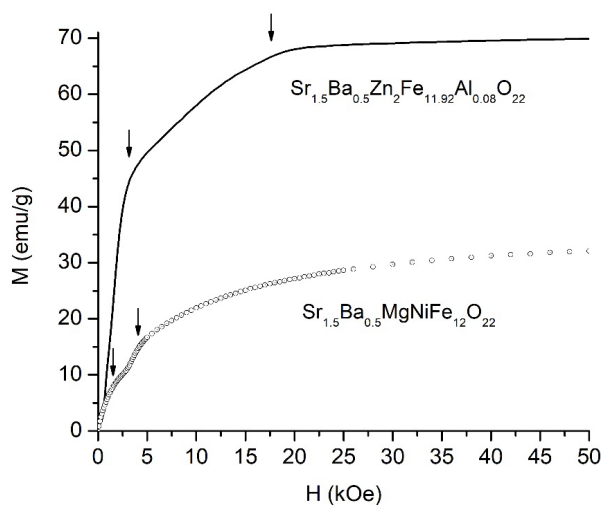
When the applied magnetic field is higher - 500 Oe, the $\text{Ba}_{0.5}\text{Sr}_{1.5}\text{Zn}_2\text{Fe}_{12}\text{O}_{22}$ sample is in a ferromagnetic state (Fig. 4a). The partial substitutions with magnetic or not magnetic cations give rise to different behavior, which indicates a change in the magnetic behavior; the

difference is significant in the case of Al substitution. The behavior of the ZFC and FC magnetization curves for a $\text{Ba}_{0.5}\text{Sr}_{1.5}\text{Zn}_2\text{Al}_{0.08}\text{Fe}_{11.92}\text{O}_{22}$ sample under a magnetic field of 500 Oe (Fig. 4a) is quite different from that at low fields (Fig. 3b). Based on the evidence obtained with single-crystal samples, the well-defined maximum at 103 K (ZFC curve) should be considered an indication that a longitudinal conical magnetic spin order sets in below this temperature. Increasing the magnetic field to 500 Oe does not affect the temperature of onset of the magnetic order transition from proper-screw to collinear ferrimagnetic one, namely, 285 K.

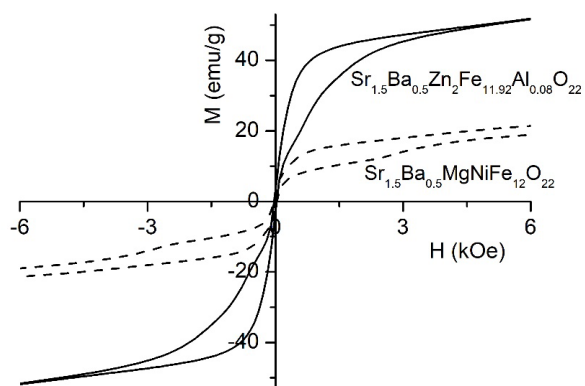
In the case of Ni substitution, the ZFC and FC magnetization curves behavior in a magnetic field of 500 Oe is quite dissimilar from those in low fields (Fig. 4b). The magnetization rises as the temperature increases. This indicates that the helical spin state can be modified further by increasing the magnetic field.

In the case of the $\text{Ba}_{0.5}\text{Sr}_{1.5}\text{NiMgFe}_{12}\text{O}_{22}$ sample, a small maximum at 27 K in the ZFC curve is observed indicating a longitudinal conical magnetic spin order at low temperature.

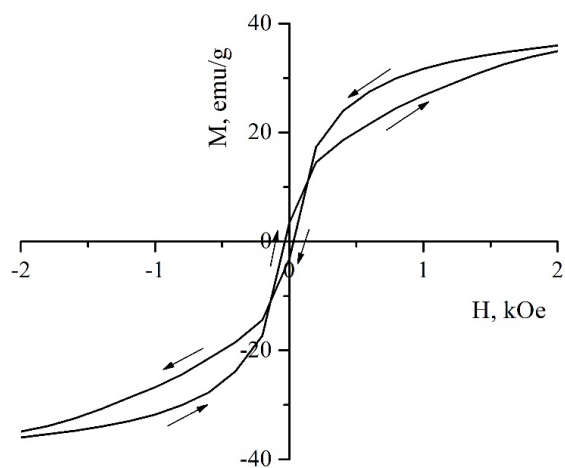
The results obtained show that the small substitution of magnetic Fe^{3+} with non-magnetic Al^{3+} leads to changes in the magnetic structure, so that a magnetic phase transition from longitudinal conical magnetic spin order to a proper-screw one and to a collinear ferrimagnetic one can be observed by changing the temperature and the magnetic field applied. In $\text{Ba}_{0.5}\text{Sr}_{1.5}\text{Zn}_{2-x}\text{Ni}_x\text{Fe}_{12}\text{O}_{22}$, the half-substitution of the non-magnetic Zn^{2+} with the magnetic Ni^{2+} shifts the helical spin screw magnetic order towards the higher temperatures. The changes in magnetic structure are due to the Ni ions preferring to occupy the octahedral



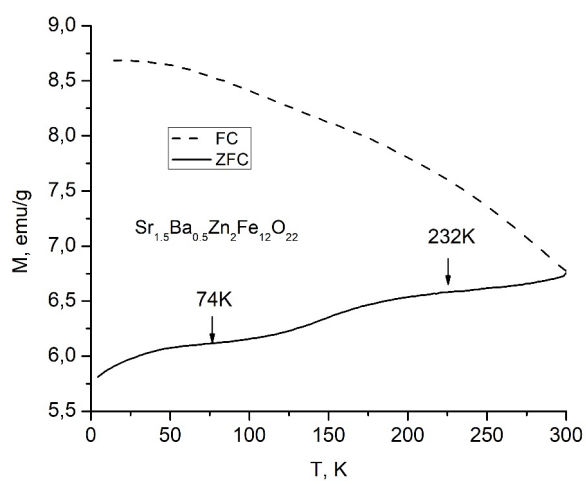
a)



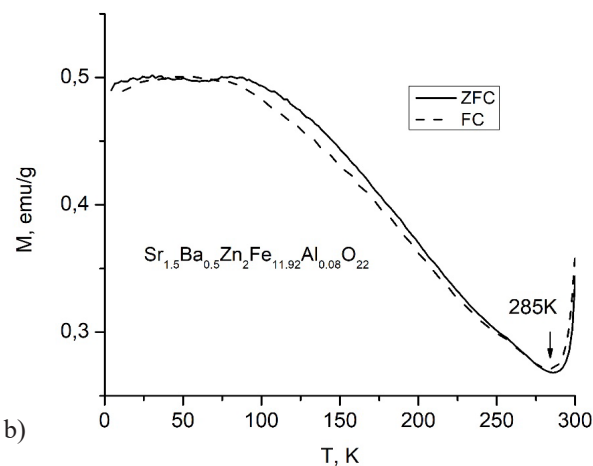
b)



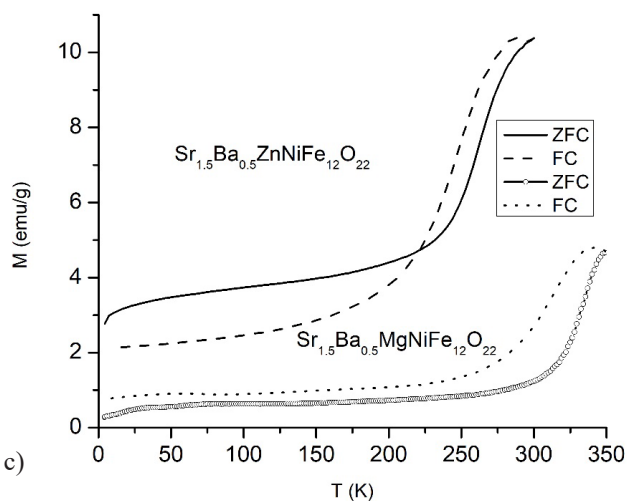
c)



a)



b)



c)

Fig. 2. (a) Initial magnetization curves of $\text{Sr}_{1.5}\text{Ba}_{0.5}\text{Zn}_2\text{Fe}_{11.92}\text{Al}_{0.08}\text{O}_{22}$ and $\text{Ba}_{0.5}\text{Sr}_{1.5}\text{NiMgFe}_{12}\text{O}_{22}$ [24] at 4.2K; (b) expanded view of the magnetization hysteresis curves at low magnetic field for $\text{Sr}_{1.5}\text{Ba}_{0.5}\text{Zn}_2\text{Fe}_{11.92}\text{Al}_{0.08}\text{O}_{22}$ and $\text{Ba}_{0.5}\text{Sr}_{1.5}\text{NiMgFe}_{12}\text{O}_{22}$ [24] at 4.2K; (c) expanded view of triple hysteresis curve for $\text{Ba}_{0.5}\text{Sr}_{1.5}\text{NiZnFe}_{12}\text{O}_{22}$ [21] at 4.2K.

Fig. 3. ZFC- and FC-magnetization vs temperature at 100 Oe: (a) $\text{Sr}_{1.5}\text{Ba}_{0.5}\text{Zn}_2\text{Fe}_{12}\text{O}_{22}$; (b) $\text{Sr}_{1.5}\text{Ba}_{0.5}\text{Zn}_2\text{Fe}_{11.92}\text{Al}_{0.08}\text{O}_{22}$ [20]; (c) $\text{Ba}_{0.5}\text{Sr}_{1.5}\text{NiZnFe}_{12}\text{O}_{22}$ and $\text{Ba}_{0.5}\text{Sr}_{1.5}\text{NiMgFe}_{12}\text{O}_{22}$ [24].

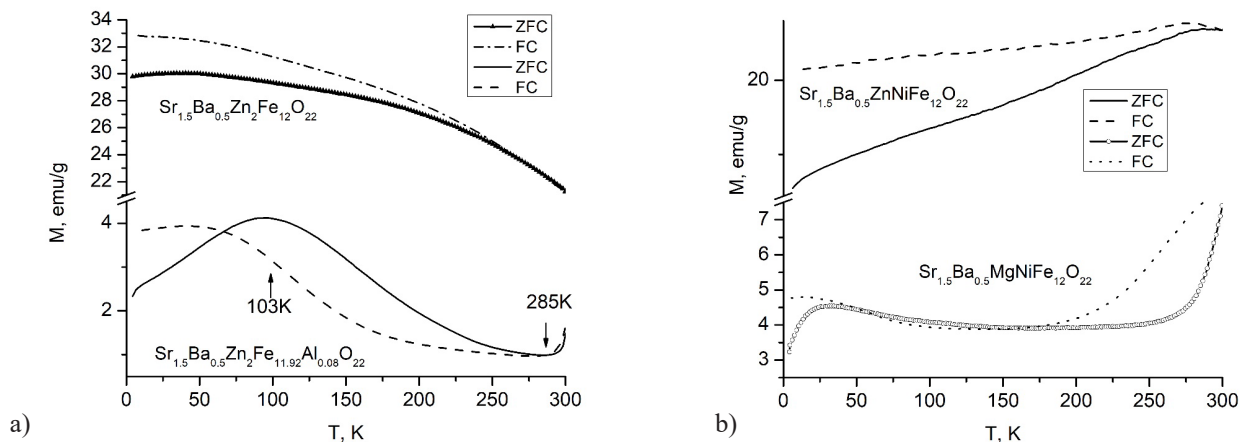


Fig. 4. ZFC- and FC-magnetization vs temperature at 500 Oe: (a) $\text{Sr}_{1.5}\text{Ba}_{0.5}\text{Zn}_2\text{Fe}_{12}\text{O}_{22}$ $\text{Sr}_{1.5}\text{Ba}_{0.5}\text{Zn}_2\text{Fe}_{11.92}\text{Al}_{0.08}\text{O}_{22}$ [20]; (b) $\text{Ba}_{0.5}\text{Sr}_{1.5}\text{NiZnFe}_{12}\text{O}_{22}$ and $\text{Ba}_{0.5}\text{Sr}_{1.5}\text{NiMgFe}_{12}\text{O}_{22}$.

positions in the crystal cell, while the Zn ions prefer the tetrahedral positions. This entails the migration of iron cations between crystallographic sites with octahedral and tetrahedral oxygen configuration and is accompanied by a corresponding change in the magnetic structure. In the case of a $\text{Ba}_{0.5}\text{Sr}_{1.5}\text{NiMgFe}_{12}\text{O}_{22}$ sample, where Mg^{2+} occupy both tetrahedral and octahedral positions, the degree of iron cations' migration between octahedral and tetrahedral crystallographic sites is smaller.

CONCLUSIONS

Studies involving magnetic measurements and allowing one to establish the magnetic phase transitions in hexaferrites are attractive in view of obtaining new knowledge on the magnetic structure of these complex materials with extraordinary properties, e.g., the existence of the magneto-electric effect. Such magnetic phase transition can be realized by varying the cation distribution in these materials' crystal structure, which results in changes in their magnetic structure in response to temperature variations. This is of great importance in obtaining materials in which large ferroelectricity and strong ferromagnetism coexist thus opening possibilities for numerous fascinating future applications.

Acknowledgements

The work was supported by the Bulgarian National Science Fund under contract KP-06-N48/5, by a joint

research project between the Bulgarian Academy of Sciences and the Institute of Low Temperature and Structure Research, Polish Academy of Sciences. Borislava Georgieva was supported by the Bulgarian Ministry of Education and Science under the National Research Programme "Young scientists and Postdoctoral students-2" approved by DCM 206/07.04.2022.

REFERENCES

1. H. Schmid, *Ferroelectrics*, 162, 1994, 317.
2. V. Kocsis, Y. Kaneko, Y. Tokunaga, Y. Tokura, Y. Taguchi, Enhanced Stability of the Multiferroic Phase in Cr-Doped Y-Type Hexaferrite Single Crystals, *Phys. Rev. Applied*, 18, 2022, 024050.
3. J. Smit, H.P.J. Wijn, *Ferrites*, Philips Technical Library, Eindhoven, 1959, p. 150.
4. T. Kimura, G. Lawes, A.P. Ramirez, Electric polarization rotation in a hexaferrite with long-wavelength magnetic structures, *Phys. Rev. Lett.*, 94, 2005, 137201.
5. S. Utsumi, D. Yoshida, N. Momozawa, Superexchange interactions of $(\text{Ba}_{1-x}\text{Sr}_x)_2\text{Zn}_2\text{Fe}_{12}\text{O}_{22}$ system studied by neutron diffraction, *J. Phys. Soc. Jpn.*, 76, 2007, 034704.
6. R.C. Pullar, Hexagonal ferrites: A review of the synthesis, properties and applications of hexaferrite ceramics, *Prog. Mater. Sci.*, 57, 2012, 1191-1334.
7. K. Taniguchi, N. Abe, S. Ohtani, H. Umetsu, T. Arima, Ferroelectric polarization reversal by a

- magnetic field in multiferroic Y-type hexaferrite $\text{Ba}_2\text{Mg}_2\text{Fe}_{12}\text{O}_{22}$, *Appl. Phys. Express*, 1, 2008, 031301.
8. K. Kouril, V. Chlan, H. Štěpánková, A. Telfah, P. Novák, K. Knížek, Y. Hiraoka, T. Kimura, Distribution of Zn in magnetoelectric Y-Type hexaferrite, *Acta Phys. Polonica A*, 118, 2010, 732-733.
 9. E.W. Gorter, Saturation Magnetization of Some Ferrimagnetic Oxides with Hexagonal Crystal Structures, *Proc. IEE - Part B: Radio and Electronic Engineering*, 104, 5S, 1957, 255-260.
 10. E. Pollert, Crystal Chemistry of Magnetic Oxides Part 2: Hexagonal Ferrites, *Prog. Cryst. Growth Charact.*, 11, 1985, 155-205.
 11. Y.S. Chai, S.H. Chun, S.Y. Haam, Y.S. Oh, I. Kim, K. H. Kim, Low-magnetic-field control of dielectric constant at room temperature realized in $\text{Ba}_{0.5}\text{Sr}_{1.5}\text{Zn}_2\text{Fe}_{12}\text{O}_{22}$, *New J. Phys.*, 11, 2009, 073030.
 12. N. Momozawa, Y. Yamaguchi, H. Takei, M. Mita, Magnetic structure of $(\text{Ba}_{1-x}\text{Sr}_x)_2\text{Zn}_2\text{Fe}_{12}\text{O}_{22}$ ($x = 0-1.0$), *J. Phys. Soc. Jap.*, 54, 1985, 771-780.
 13. N. Momozawa, Neutron Diffraction Study of Helimagnet $(\text{Ba}_{1-x}\text{Sr}_x)_2\text{Zn}_2\text{Fe}_{12}\text{O}_{22}$, *J. Phys. Soc. Jpn.*, 55, 1986, 4007-4013.
 14. S. Hirose, D. Urushihara, T. Asaka, T. Kimura, Improved room-temperature magnetoelectric effect and crystal structure in polycrystalline $\text{BaSrCo}_2\text{Fe}_{11}\text{AlO}_{22}$, *Appl. Phys. Lett.*, 118, 2021, 062407.
 15. V.A Zhuravlev, D.V. Wagner, O.A. Dotsenko, K.V. Kareva, E.V. Zhuravlyova, A.S. Chervinskaya, G.E. Kuleshov, A.S. Suraev, www Static and Dynamic Magnetic Properties of Polycrystalline Hexaferrites of the $\text{Ba}_2\text{Ni}_{2-x}\text{Cu}_x\text{Fe}_{12}\text{O}_{22}$ System, *Electronics* 2022, 11, 2759.
 16. Xi Deng, Yijing Chen, Zhiwen Shi, Han Liu, Tao Wen, Huihong Wu, Linqiang Xie, Zhenzhi Cheng, Guangsheng Luo, Weiping Zhou, Cr^{3+} doping-controlled magnetic and dielectric properties of polycrystalline Y-type $\text{BaSrCo}_2\text{Fe}_{11-x}\text{Cr}_x\text{AlO}_{22}$ hexaferrite, *J. Magn. Mater.* 586, 2023, 171166.
 17. M. Arshad, M. A.Khan, Gh. A. Ashraf, K. Mahmood, K. I. Arshad, Investigation of crystal structure, electrical and dielectric response of Zr^{4+} - Co^{2+} substituted Ba-Sr-Ni Y-type hexagonal ferrites synthesized by sol-gel route, *Ceram. Int.*, 49, 2023, 4141-4152.
 18. M. Suthar, A.K. De, A. Indra, I. Sinha, P.K. Roy, Synthesis and characterization of titanium-substituted nanocrystalline Co_2 -Y hexaferrite: magnetically retrievable photocatalyst for treatment of methyl orange contaminated wastewater, *Environ. Sci. Pollut. Res.*, 30, 2023, 44457-44479.
 19. B. Georgieva, S. Kolev, K. Krezhov, Ch. Ghelev, D. Kovacheva, B. Vertruyen, R. Closset, L.M. Tran, M. Babij, A.J. Zaleski, T. Koutzarova, Structural and magnetic characterization of Y-type hexaferrite powders prepared by sol-gel auto-combustion and sonochemistry, *J. Magn. Mater.*, 477, 2019, 131-135.
 20. B. Georgieva, S. Kolev, K. Krezhov, Ch. Ghelev, D. Kovacheva, L.M. Tran, M. Babij, A. Zaleski, B. Vertruyen, R. Closset, T. Koutzarova, Magnetic phase transitions in $\text{Ba}_{0.5}\text{Sr}_{1.5}\text{Zn}_2\text{Fe}_{11.92}\text{Al}_{0.08}\text{O}_{22}$ hexaferrites, *J. Phys. Conf. Ser.*, 1762, 2021, 012034.
 21. T. Koutzarova, S. Kolev, K. Krezhov, B. Georgieva, Ch. Ghelev, D. Kovacheva, B. Vertruyen, R. Closset, L.M. Tran, M. Babij, A.J. Zaleski, Ni-substitution effect on the properties of $\text{Ba}_{0.5}\text{Sr}_{1.5}\text{Zn}_{2-x}\text{Ni}_x\text{Fe}_{12}\text{O}_{22}$ powders, *J. Magn. Mater.*, 505, 2020, 166725.
 22. J. Kim, H. Choi, Ch. S. Kim, Magnetic properties of polycrystalline Y-type hexaferrite $\text{Ba}_{2-x}\text{Sr}_x\text{Ni}_2(\text{Fe}_{1-y}\text{Al}_y)_{12}\text{O}_{22}$ using Mössbauer spectroscopy, *AIP Advances* 10, 2020, 015204.
 23. S. Kolev, B. Georgieva, T. Koutzarova, K. Krezhov, Ch. Ghelev, D. Kovacheva, B. Vertruyen, R. Closset, L.M. Tran, M. Babij, A.J. Zaleski, Magnetic Field Influence on the Microwave Characteristics of Composite Samples Based on Polycrystalline Y-Type Hexaferrite, *Polymers*, 14, 2022, 4114.
 24. B. Georgieva, S. Kolev, Ch. Ghelev, K. Krezhov, D. Kovacheva, B. Vertruyen, R. Closset, L.M. Tran, M. Babij, A. Zaleski, T. Koutzarova, Effect of cation substitutions in Y-type $\text{Ba}_{0.5}\text{Sr}_{1.5}\text{Me}_2\text{Fe}_{12}\text{O}_{22}$ hexaferrites on the magnetic phase transitions, *J. Phys. Conf. Ser.*, 2240, 2022, 012023.
 25. Y. Hiraoka, H. Nakamura, M. Soda, Y. Wakabayashi, T. Kimura, Magnetic and magnetoelectric properties of $\text{Ba}_{2-x}\text{Sr}_x\text{Ni}_2\text{Fe}_{12}\text{O}_{22}$ single crystals with Y-type hexaferrite structure, *J. Appl. Phys.*, 110, 2011, 033920.
 26. T. Koutzarova, S. Kolev, K. Krezhov, B. Georgieva, Phase transitions in magneto-electric hexaferrites, *ACS Omega*, 7, 2022, 44485-44494.